Title: Ribosome demand links transcriptional bursts to protein expression noise

Authors: Sampriti Pal[1], Upasana Ray[1], Riddhiman Dhar[1]*

Affiliations:

[1]Department of Bioscience and Biotechnology, IIT Kharagpur, India

*Corresponding author. Email: riddhiman.dhar@iitkgp.ac.in

Stochastic variation in protein expression generates phenotypic heterogeneity in a cell population and has an important role in antibiotic persistence, mutation penetrance, tumor growth and therapy resistance. Studies investigating molecular origins of noise have predominantly focused on the transcription process. However, the noise generated in the transcription process is further modulated by translation. This influences the expression noise at the protein level which eventually determines the extent of phenotypic heterogeneity in a cell population. Studies across different organisms have revealed a positive association between translational efficiency and protein noise. However, the molecular basis of this association has remained unknown. In this work, through stochastic modeling of translation in single mRNA molecules and empirical measurements of protein noise, we show that ribosome demand associated with high translational efficiency in a gene drives the correlation between translational efficiency and protein noise. We also show that this correlation is present only in genes with bursty transcription. Thus, our work reveals the molecular basis of how coding sequence of genes, along with their promoters, can regulate noise. These findings have important implications for investigating protein noise and phenotypic heterogeneity across biological systems.

Running Title: Translational control of gene expression noise

Keywords:

Protein expression noise; Transcriptional bursts; Translational bursts; Translational efficiency; Ribosome demand

Introduction

Genetically identical cells often show variation in gene expression under identical environmental condition. Stochastic variation in gene expression, termed as expression noise, generates phenotypic heterogeneity which has important implications for many biological processes. Gene expression noise has been associated with persistence of microbial cells in antibiotics[1,2], incomplete mutation penetrance[3-5], cellular decision-making[6,7], cancer progression, and anti-cancer therapy resistance[8-10]. Transcription occurring in bursts[11-13], with a promoter transitioning between on- and off-states, is a major source of expression noise, and each promoter has its characteristic burst frequency and burst size[14-18]. Earlier studies have associated presence of TATA box motif[19,20], occurrence of TFIID and SAGA co-activator complexes with TATA binding protein [21], nucleosome occupancy, and histone modifications with expression noise[22-25]. In addition, transcription factors (TFs) and gene regulatory networks play important roles in determining noise [26-28].

The expression noise generated by transcription is modulated by the translation process[13,29]. Thus, a gene that exhibits high expression noise at the mRNA level may not show high noise at the protein level. Two early studies observed a positive association between translational efficiency and expression noise in bacteria and yeast[30,31], where an increase in mean protein expression, engineered by changes in synonymous codons, led to an increase in expression noise. This contrasted with the traditional inverse relationship between mean protein expression and noise observed in empirical measurements of noise in bacteria and yeast[14-16]. Salari *et al.*[32], through a computational analysis of expression noise in yeast, observed an increase in positive correlation between tRNA adaptation index (tAI), a proxy for translational efficiency[33,34], and

expression noise for genes with tAI up to 0.55. The correlation, however, decreased thereafter[32]. In addition, a recent study in *Arabidopsis* reported a positive correlation between translational efficiency and expression noise[35], similar to what had been observed in microbes. Taken together, these studies showed that the translation process impacted protein expression noise in similar manner across biological systems.

What is the molecular basis of the positive correlation between translational efficiency and protein expression noise? The answer to this question remains unclear, although some mechanisms have been proposed. To achieve a specific protein expression level, a cell can produce many mRNA molecules and translate them at a low rate, or can start with a small number of mRNA molecules and translate them at a high rate[36]. It has been argued that the latter scenario requiring high translation rate may lead to more noise, due to constraints on availability of mRNA, or due to fluctuations in small mRNA numbers[36,37]. However, there has only been indirect evidence in support of this hypothesis[36]. Further, recent studies have shown that the translation process is bursty in nature and can switch between on- and off-states[38,39], just like the transcription process. Whether translational bursting along with transcriptional bursts can explain the correlation between translational efficiency and noise remains unknown.

In this work, we show that fluctuations in mRNA levels, originating from bursty transcription, combined with high translational efficiency can lead to high protein noise. Through stochastic modeling of translation in single mRNA molecules, we uncovered that the extent of demand for the ribosomal machinery needed for translation at the level of individual genes determined how transcriptional noise was translated into protein noise. In addition, we found that the positive association between translational efficiency and protein noise was visible only for genes that

showed bursty transcription. Consequently, the ribosome demand model predicted that a reduction in translational efficiency or a departure from bursty transcription to a more uniform rate of transcription would abolish the association between translational efficiency and protein noise. We validated both these predictions through an experimental noise measurement system in yeast, thereby establishing ribosome demand as the molecular link between transcriptional bursts and protein noise. Taken together, our work reveals the molecular basis of how coding sequence of genes can regulate protein noise via modulating the translation rate. These findings have implications for investigating protein noise and phenotypic heterogeneity across biological systems.

Results

High protein noise in genes with low transcription and high translation stems from high mRNA noise

We first tested the existing hypothesis which posits that genes with low transcription and high translation will exhibit more protein expression noise than the genes with high transcription and low translation (Fig. 1A). Although it has been reported that essential genes in the yeast *Saccharomyces cerevisiae* employ high transcription and low translation strategy for expression, presumably because of detrimental effects of high noise in these genes[36], there is no direct supportive evidence. To directly test this hypothesis, we compared protein expression noise of genes showing different levels of transcription and translation in the yeast *S. cerevisiae*. We obtained the mRNA expression data from the study of Nadal-Ribelles *et al.*[40], who quantified mRNA expression at the level of single cells in yeast (Fig. S1A). We used the protein synthesis rate per mRNA data from Riba *et al.*[41] as a measure of translational efficiency (Fig. S1B). We obtained the protein expression noise data from Newman *et al.*[15], and used their measure of

Distance-to-Median (DM) that is corrected for the dependence of expression noise (coefficient of variation, CV) on mean protein expression. We obtained protein noise values of 2763 genes from this dataset (Fig. S1C).

Mean mRNA expression and translational efficiency individually showed poor correlation with protein noise (Fig. S2). We therefore classified yeast genes based on the quartiles of mean mRNA expression values, and then by the quartiles of translational efficiency resulting in a total of 16 classes (Fig. 1B). The group of genes with low mRNA expression and high translational efficiency showed more than ten-fold increase in protein noise (DM) compared to the genes with high mRNA expression and low translational efficiency (Mann-Whitney U-test, p=0.001; Fig. 1B), suggesting that low mRNA expression and high translational efficiency was indeed associated with high protein noise.

To better understand how low mRNA expression and high translational efficiency could lead to high protein noise, we employed a two-state model of gene expression[42]. Briefly, a gene can switch between on- and off-states with rates K_{on} and K_{off}, respectively (Fig. 1C). In the on-state, the gene is transcribed at a rate β_m, and the mRNA molecules produced are translated at a rate β_p. Using stochastic simulations following Gillespie's algorithm[43], we modeled the changes in concentrations of mRNA and protein molecules over time in each of 1000 cells, and further calculated mean protein expression and noise values (coefficient of variation, CV) (see Methods). We modeled the impact of mRNA expression and translational efficiency on expression noise by varying the transcription (β_m) and the translation (β_p) rates over a wide range of values (Fig. 1D). However, we did not see any change in protein noise, either with changes in the translation rate for a specific mean mRNA expression, or with changes in the mean mRNA

expression (CV= ~0.62, Fig. 1D). Further, simulations over a wide-range of burst frequencies (K_{on}) did not reveal any correlation between translation rate and protein noise (Fig. 1E). These results suggested that the differences in initial mRNA numbers and the translation rates could not explain the differences in noise values between low-mRNA high-translation class compared to the high-mRNA low-translation class.

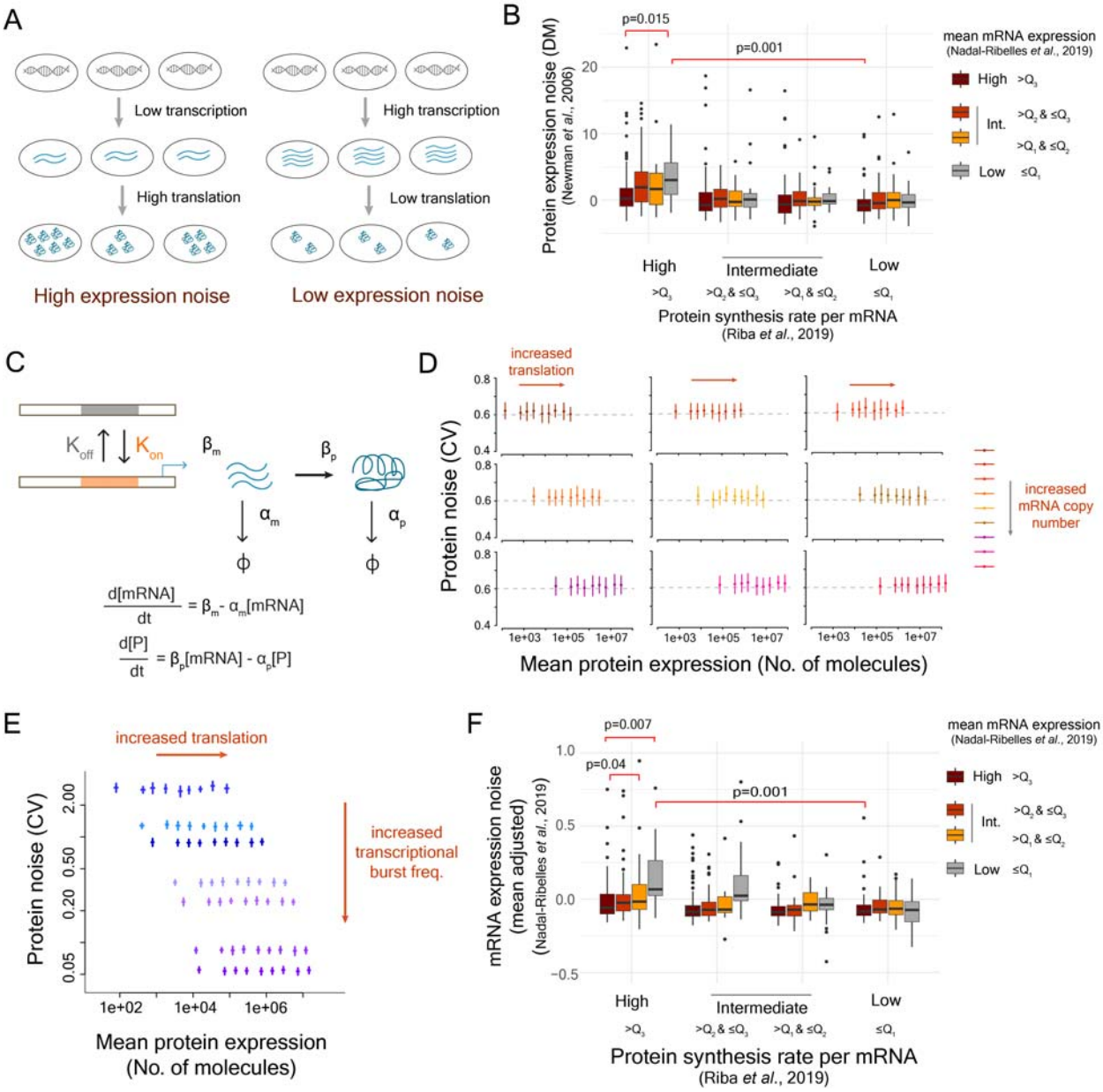

Fig. 1. High mRNA noise combined with high translational efficiency leads to high protein noise (A) Existing model to describe impact of translational efficiency on protein expression noise. **(B)** Protein noise among 16 classes of genes classified according to the quartiles of mean mRNA expression, calculated from Nadal-Ribelles *et al.*[40], and then by the quartiles of protein synthesis rates per mRNA from Riba *et al.*[41]. **(C)** Two-state model of gene expression with the transition rates K_{on} and K_{off}. **(D-E)** Relationship between mean protein expression and protein noise (CV) obtained from stochastic modeling at different transcription rates (D) and at different transcriptional burst frequencies (E) **(F)** Mean-adjusted mRNA expression noise calculated from the single-cell RNA-seq data[40] in 16 classes of genes classified according to the quartiles of mean mRNA expression and the quartiles of protein synthesis rate per mRNA. Q_1, Q_2, and Q_3 represent first, second and third quartiles.

Next, we tested whether higher heterogeneity in mRNA numbers of genes with low mean mRNA expression could explain the higher protein noise in the low-mRNA high-translation class[37]. To do so, we derived a measure of mean-adjusted mRNA expression noise[28] for 5475 genes from yeast single-cell RNA-seq data[40] (Fig. S3A,B). In general, the genes with low mean mRNA expression showed high mean-adjusted mRNA expression noise (Fig. S3C). Next, we compared mRNA expression noise in the 16 classes of genes obtained earlier according to the levels of mean mRNA expression and protein synthesis rate (Fig. 1B). The class of genes with low mean mRNA expression and high translational efficiency showed the highest mRNA noise among all classes (Fig. 1F). Specifically, this class of genes had more than 37-fold higher absolute mRNA noise value (mean mRNA noise = 0.165) compared to the class with high mRNA level and low translational efficiency (mean mRNA noise = -0.0044) (Mann-Whitney U-test, p=0.001, Fig. 1F). In general, protein expression noise showed a moderate correlation with mRNA noise (Pearson's correlation = 0.44 and Spearman's correlation = 0.29, Fig. S3D). These results suggested that high mRNA noise associated with low transcription, rather than the low mean mRNA expression itself, combined with translational efficiency was a good determinant of protein noise.

Bursty transcription combined with high translational efficiency leads to high protein noise

Based on the above observations, we put forward a new working model that highlighted the influence of mRNA noise in determining protein noise. Noise in mRNA expression is usually associated with bursty transcription, where low burst frequency leads to high mRNA expression noise and an increase in burst frequency gradually lowers mRNA noise as the transcription rate becomes more uniform. Therefore, we hypothesized that among genes that exhibited bursty transcription, the ones with high translation rate would show higher protein noise compared to the ones with low translation rate (Fig. 2A).

To test this new model, we estimated the parameters associated with transcriptional bursts such as on- and off- transition rates (K_{on} and K_{off}) and transcription rate (β_m) for >6000 genes in yeast from single-cell RNA-seq data (Fig. S4)[40], using a maximum-likelihood approach based on a Poisson-Beta model[44] (Fig. 2B). Genes with low transcriptional burst frequencies showed high mRNA noise (Fig. S5). However, the genes that exhibited high protein noise were associated with high translational efficiency (Fig. 2C). In addition, we classified genes into 16 classes according to the quartiles of burst frequency and the quartiles of translational efficiency (Fig. 2D). Genes with low burst frequency and high translational efficiency showed highest protein noise among all 16 classes (Fig. 2D). This class of genes showed a mean protein noise (DM) value of 5.65, whereas, the class of genes with high burst frequency and high protein synthesis rate showed a mean protein noise (DM) value of -0.038 (Mann-Whitney U test, $p=1.22 \times 10^{-7}$; Fig. 2D). These observations confirmed that high translation rate, combined with bursty transcription, could lead to high protein noise (Fig. 2D). Analysis with tAI as the measure of translational efficiency showed similar trend (Fig. S6, S7), suggesting that these results were robust to use of different measures of translational efficiency.

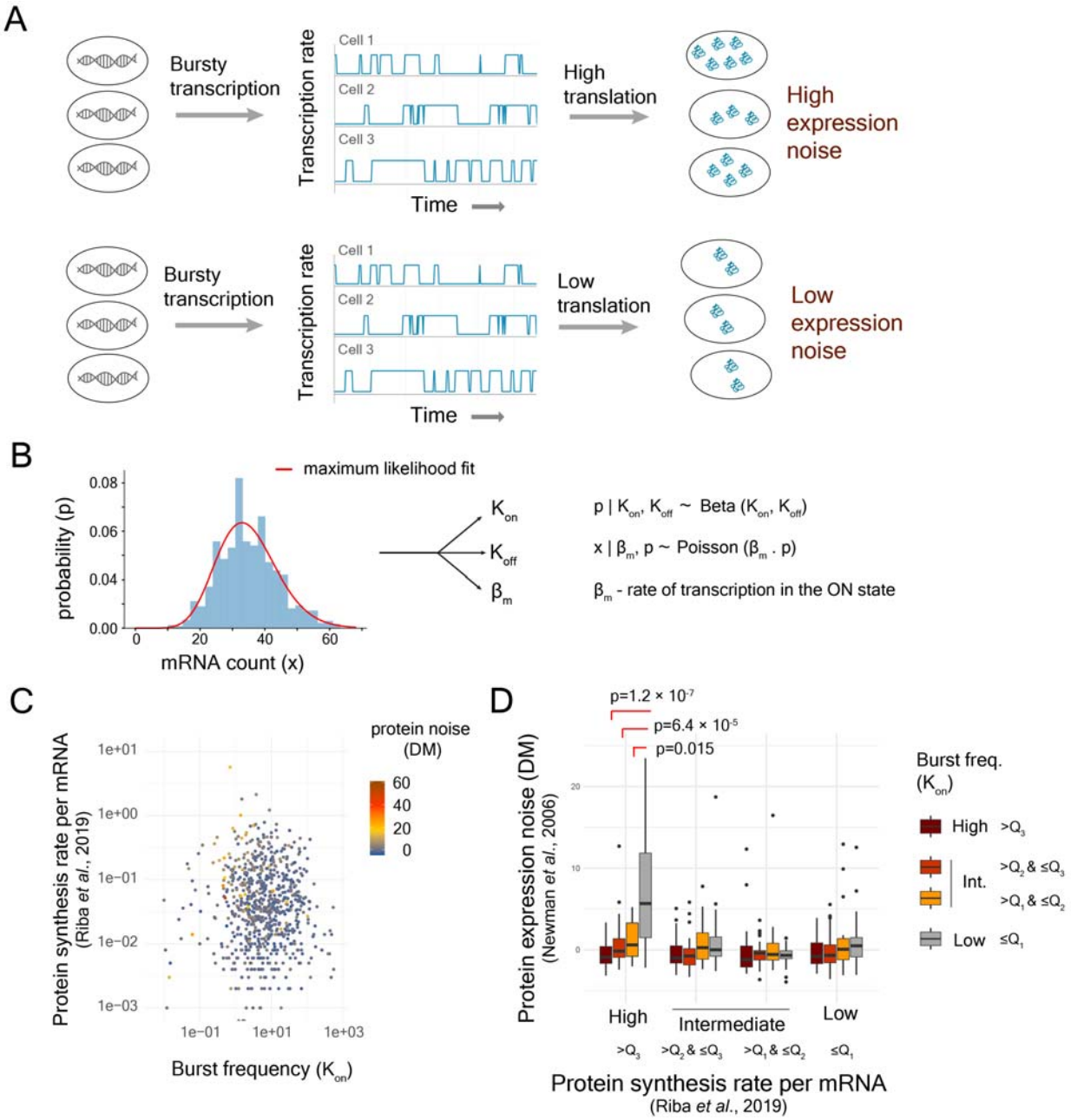

Fig. 2. Stochastic fluctuation in mRNA expression, originating from transcriptional bursts, combined with high translational efficiency generates high protein noise. (A) The new working model **(B)** Estimation of parameters of two-state model of gene expression from single-cell RNA-seq data **(C)** Protein noise of genes with different levels of transcriptional burst frequencies and protein synthesis rates per mRNA **(D)** Protein noise (DM) of genes classified into 16 classes based on burst frequency and protein synthesis rate per mRNA. Q_1, Q_2, and Q_3 represent first, second and third quartiles.

Bursty translation does not explain the correlation between translational efficiency and protein noise

Even though results from the analysis of available data were in agreement with the new working model, it did not explain how high translational efficiency combined with low burst frequency could lead to high protein noise, and how reducing translational efficiency could lower protein noise. Recent studies have observed that translation, like transcription, also occurs in bursts[38,39]. Specifically, Livingstone *et al.* [39], through single-cell mRNA tracking, measured the parameters of translational bursting and identified the roles of 5'UTR and 5'mRNA cap in modulation of translational burst frequency and burst amplitude.

Therefore, we asked whether incorporating translational bursting into our model could uncover the positive correlation between translational efficiency and protein noise. To do so, we built a TASEP based model[45-46] of translation, with appropriate modifications, at the level of single mRNA molecules (Fig. 3A, see Methods). We assumed that an mRNA molecule could transition between on- and off-states[39] with rates TL_{on} and TL_{off}, respectively, and in the on-state, translation initiation occurred at the rate of TL_{init} (Fig. 3A). As multiple ribosomes could translate a single mRNA molecule at the same time, a second translation initiation happened only when the preceding ribosome traversed at least 10 codons, to account for steric interaction between ribosomes[47,48] (Fig. 3B). Several earlier studies have showed the presence of a gradually increasing profile of translational efficiency or ramp, even though to different degree, in the 5' end of coding regions of genes[34,49]. This meant that the translation speed was lower near the 5' end of a gene and the speed gradually increased as ribosome traversed from 5' to 3' end of an mRNA molecule. Taking this into account, we modeled the traversal speed of the ribosomes

using a first-order Hill function where the traversal speed was dependent on the position of the ribosome in the codon (Fig. 3B). An increase in the value of the parameter K_{Hill} led to an increased traversal time (Fig. 3C). The speed of traversal can also impact translation initiation rate, as observed by Barrington *et al.*[50], this meant that K_{Hill} was also related to the translation initiation rate TL_{init}. Higher translation initiation rate necessitated lower K_{Hill} to ensure faster traversal of the preceding ribosome through first 10 codons to avoid collision between two successive ribosomes (Fig. 3D). Similarly, lower K_{Hill} value permitted a greater number of translation initiation events per unit time (Fig. 3D). Thus, higher translation rate in turn meant shorter traversal time for a ribosome through the gene (Fig. 3D).

We integrated the model of translation with the two-state model of transcription, and performed stochastic simulations in 1000 cells to estimate mean protein expression and protein noise (coefficient of variation, CV). For all transcriptional burst frequencies examined, we did not observe any change in protein noise with an increase in translation initiation rate (Fig. 3E). We also tested the model at different translational burst frequencies. Although changes in translational burst frequencies altered the level of protein noise, we did not find any correlation between mean expression and protein noise (Fig. 3F). These results suggested that a simple model integrating transcriptional and translational bursting could not explain the observed relationship between translational efficiency and protein noise.

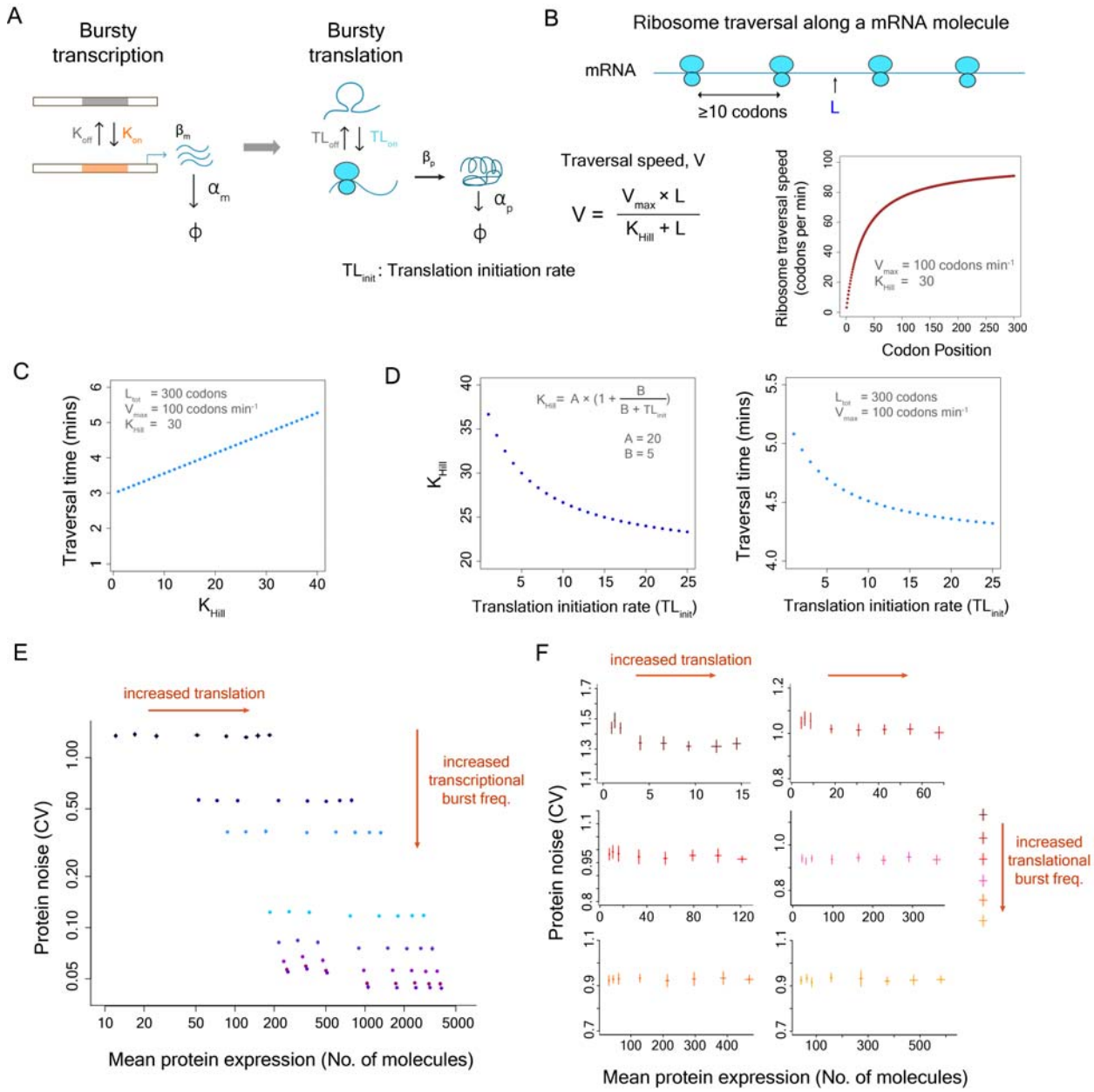

Fig. 3. The model combining transcriptional and translational bursts does not explain the correlation between translational efficiency and protein noise (A) Integrated model of translational and transcriptional bursts **(B)** Ribosomal traversal speed along an mRNA molecule and the traversal speed is given by V at a position L in the mRNA molecule. **(C)** Traversal time as a function of K_{Hill} **(D)** Relationship between K_{Hill}, translation initiation rate and ribosome traversal time. A and B are parameters of the model. **(E)** Changes in protein noise with changes in translation rate and transcriptional burst frequency **(F)** Changes in protein noise with changes in translation rate and translational burst frequency.

Inclusion of ribosome demand reveals a correlation between translational efficiency and protein noise

Next, we analyzed several molecular models that could possibly explain the positive correlation between translational efficiency and protein noise. An increase in translational efficiency, leading to a higher translation rate, will require an increased supply of tRNA molecules and ribosomes. Could an increase in translation rate lead to a bottleneck in supply of tRNA, and generate variation in protein expression across cells? This seemed highly unlikely, as high translation rate is associated with presence of preferred codons, for which abundant tRNA molecules are available in a cell[33,34]. In comparison, rare codons have lower numbers of corresponding tRNA molecules available[33,34]. Thus, presence of rare codons would, in fact, cause a bottleneck in tRNA supply and hence, could cause higher expression noise. This would further imply that a reduction in translation efficiency would generate higher expression noise, which would contradict the actual empirical observations[30,31].

The translation rate is dependent on availability of ribosome machinery in the cell. We analyzed whether higher rate of translation could lead to a bottleneck in the availability of ribosomes for an mRNA, cause variation in the translation process of a gene among individual cells and thereby, generate high expression noise. It has been reported that competition for ribosomes rather than tRNA, imposes constraints on translation in yeast[51]. In addition, studies in cell-free systems have shown that constraints on resources for transcription and translation can cause bursty expression[52].

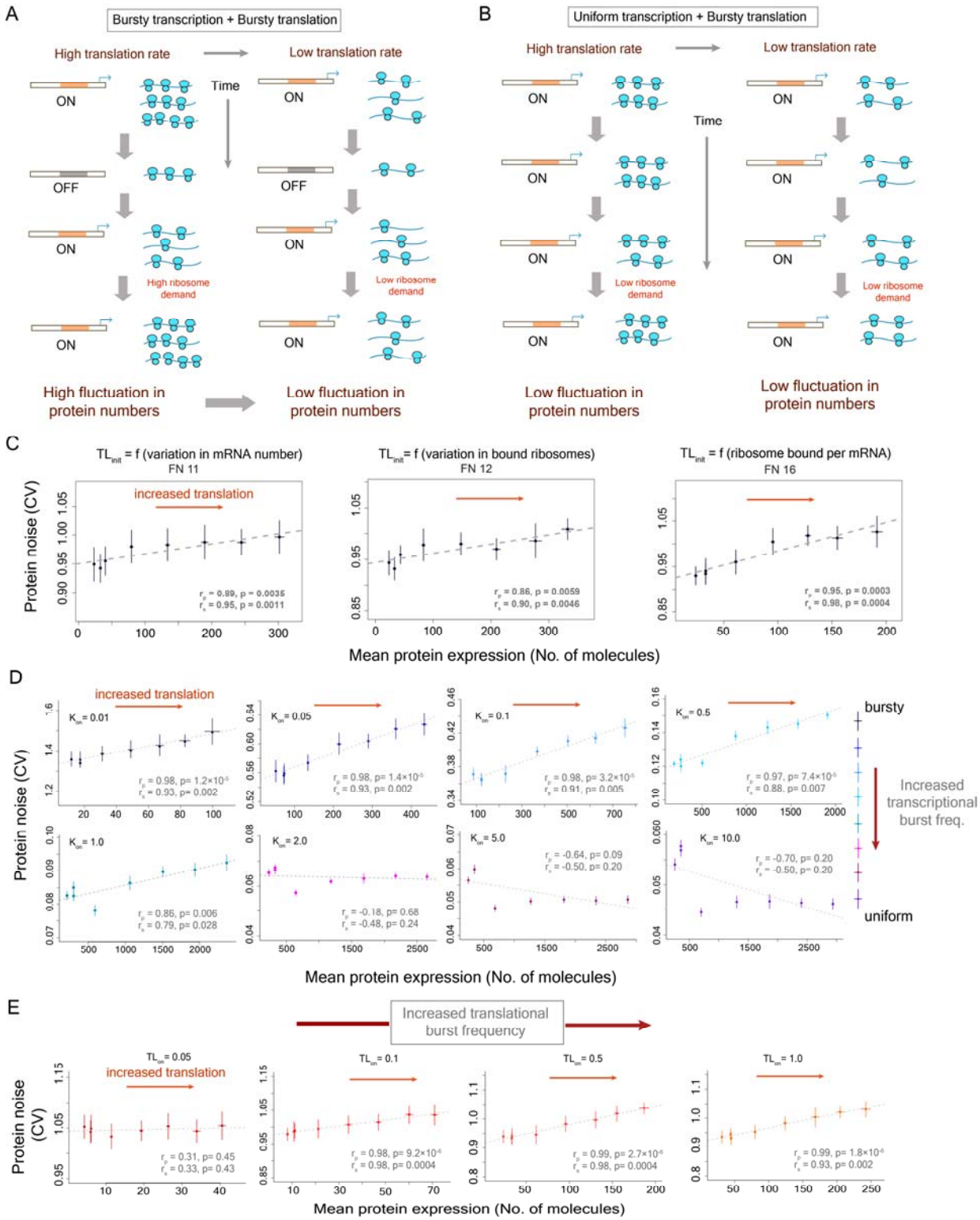

Fig. 4. Inclusion of ribosome demand associated with translation can reveal positive correlation between translational efficiency and protein noise (A) Variation in ribosome demand with bursty transcription and bursty translation **(B)** Ribosome demand with uniform transcription and bursty translation **(C)** Functions to model the impact of ribosome demand on

translation rate (Table S1 and Fig. S8) **(D-E)** Changes in protein noise with an increase in translation rate, at different transcriptional burst frequencies (D), and at different translational burst frequencies (E).

For a gene that is transcribed in bursts, there will be considerable temporal fluctuation in the number of mRNA molecules available for translation. When the mRNA copy number is high, they will require many ribosomes for translation. As the mRNA copy number drops due to stochastic fluctuations in transcription rate, some of the ribosomes earlier involved in translation of mRNA molecules of this gene become available, and can be allocated for translating mRNA molecules of other genes (Fig. 4A). At a subsequent time-point when the mRNA number of this gene rises again, it increases the demand for ribosomes (Fig. 4A). In actively growing cells, where the demand for ribosomal machinery is high, this can constrain translation initiation rate for these mRNA molecules. As the allocation of ribosomes to mRNA molecules is likely to be a stochastic process, this can generate variation in translation rates and consequently, protein expression between cells.

There are two predictions that come out of this model. First, it predicts that a reduction in the high demand for ribosome machinery during the low- to high- mRNA transition will lower protein expression noise (Fig. 4A). This can be achieved by lowering the translational efficiency of the gene, resulting in lower translation rate per mRNA. In this scenario, we will observe high protein noise at high translation rate and low noise at low translation rate, which will be in agreement with the empirical observations.

Another way of minimizing the sudden demand for ribosomes is to reduce temporal fluctuations in mRNA numbers. This can be achieved at the level of transcription by employing a more uniform rate of transcription (Fig. 4B). Thus, according to the second prediction, protein noise of

genes that are expressed in a uniform rate of transcription will be minimally affected by changes in the translation rate (Fig. 4B).

In addition, we explored whether co-translational protein folding, ribosome collision, translational errors, or changes in mRNA stability associated with translation rate could explain the positive association between translational efficiency and protein noise. Proteins are co-translationally folded as they exit through the ribosome tunnel after translation[53]. The speed of translation might affect the efficiency of co-translational folding, and perhaps, fast translation could lower efficiency of co-translational folding. This can generate misfolded proteins that are degraded. Since this process is stochastic in nature, it can lead to increased variation in protein expression among cells within a population. However, several studies have reported the exactly opposite phenomenon. A study by Spencer *et al.*[54] showed that the use of optimal codons leads to better folding of the encoded polypeptide. Other studies have shown that fast translation can in fact help avoid misfolded states, and can help in better co-translational folding, especially for misfolding-prone regions[55,56].

Fast translation means fast traversal of ribosomes through an mRNA molecule. This means higher ribosomal density on an mRNA molecule, and a higher chance of collision between two successive ribosomes on the same mRNA molecule. Slower translation puts ribosomes further apart from each other, thereby lowering the chance of ribosome collision. Ribosome collision leads to degradation of mRNA, rescue of bound ribosome and can also affect further translation initiation[57-59]. Therefore, this could be a possible reason for higher protein noise in genes that show high translation rate. However, in contrast to the ribosome demand model, this observation would hold for all genes with high translation rate, irrespective of their burst frequencies.

We further considered whether translational errors could explain the correlation between translation rate and protein expression noise. It is possible that fast translation can lead to more translational errors. This can generate proteins with wrong amino acids, which can result in protein misfolding and therefore, can lead to protein degradation. Since translational errors occur at random, this process will vary from one cell to another, which can lead to higher protein expression noise. However, there are conflicting reports regarding this. An earlier study reported that translational errors occurred at sites where the speed of ribosome was higher[60]. On the other hand, a recent study observed that preferred or optimal synonymous codons were translated more accurately[61].

Finally, we also considered whether the translation process itself could change mRNA stability and therefore, could generate cell-to-cell variation. It has been reported that increased translation can lead to higher mRNA destabilization[62]. In addition, codon optimality and thus elongation rate has also been suggested to be positively associated with mRNA stability[63]. A more recent study has however showed that translation initiation rate, but not elongation rate, is the major determinant of mRNA stability and inhibition of translation initiation has been shown to increase mRNA decay[64]. However, if changes in the translation rates altered mRNA stability and led to increased variation in cell-to-cell variation in protein concentration, this will be observed for all genes irrespective of their burst characteristics.

Since the ribosome demand model agreed with the earlier empirical observations, we tested whether incorporating ribosome demand in our mathematical model of translation could capture the observed positive association between translation efficiency and protein noise. To model demand, we tested various mathematical functions. The translation initiation rate (TL_{init}) was

considered a function of variation in mRNA number, variation in number of bound ribosomes, and variation in ribosome bound per mRNA molecule (Fig. 4C, Fig. S8). Interestingly, the functions where translation initiation rate was dependent on the number of ribosomes bound per mRNA molecule showed the most positive association between mean protein expression and protein noise (Fig. 4C, Fig. S8). We, therefore, considered one of these functions (function 16) for all subsequent analysis (Fig. 4C, Table S1). However, we observed similar positive association for several variants of these functions suggesting that the association found was robust to variations in the actual form of the function (Table S1, Fig. S8).

To further test whether our mathematical model could capture the two predictions of the ribosome demand model, we performed stochastic simulations for a wide range of transcriptional and translational burst frequencies (Fig. 4D). At low transcriptional burst frequencies, protein noise increased with an increase in translation rate (Fig. 4D). In addition, as we increased the transcriptional burst frequency and moved towards a more uniform rate of transcription, the translation rate had minimal effect on protein noise (Fig. 4D). Thus, the mathematical model could recapitulate both predictions of the ribosome demand model.

We also tested the impact of translational burst frequency on the association between translational efficiency and protein noise (Fig. 4E). At very low translational burst frequencies, protein noise did not show much change with an increase in translation rate (Fig. 4E). This was due to very low level of protein production at very low translational burst frequency, as mRNA molecule mostly resided in the inactive state. At higher translational burst frequencies, we again observed an increase in protein noise with an increase in the translation rate and hence with an increase in mean protein expression (Fig. 4E). We further tested the robustness of our stochastic

modeling approach through a systematic variation in values of several model parameters (Fig. S9-S15), as well as explored different scenarios through random sampling of the parameter space (Fig. S16).

Impact of coding sequence mutations on protein noise is dependent on the burst characteristics of the promoter

To empirically test the predictions of the ribosome demand model, we set up an experimental assay to measure protein expression noise in the yeast model system (Fig. 5A). We built gene constructs where the expression of a green fluorescent protein (*GFP*) gene could be controlled by different promoters with different burst frequencies (Fig. S17). We then introduced several mutant variants of the GFP gene with altered translational efficiencies, under the regulation of these promoters. We integrated all constructs into the yeast genome, to eliminate expression noise arising from fluctuations in plasmid copy number (Fig. 5A). We measured GFP expression using flow cytometry (Fig. S18), and estimated noise from a homogeneous group of cells that showed very similar cell size and cell complexity[14] (Fig.5B, Fig. S19).

We picked four promoters for our constructs (Fig. 5C) - two promoters, of *RPG1* and *RPL35A* genes, with high burst frequencies (K_{on}=22.855 and K_{on}=47.464 respectively) and low protein noise (DM=-0.841 and DM=-1.4 respectively)[15], and two promoters, of *CPA2* and *QCR2* genes, with low burst frequencies (K_{on}=0.704 and K_{on}=1.186 respectively) and high protein noise (DM=9.583 and DM=3.515 respectively). Our measurements also confirmed that the promoters *CPA2* and *QCR2* had higher protein noise compared to *RPG1* and *RPL35A* (Fig. 5D).

To change translational efficiency in all gene constructs in a similar manner, we built variants of the GFP gene that differed in their codon usage. This altered the translation elongation rate which in turn would also alter the translation initiation rate[50]. We constructed seven mutant variants of the *GFP* gene and cloned each of them under the control of these four promoters. The variants consisted of seven single mutants and two variants with multiple mutations. Many of the codon substitutions led to usage of nonpreferred codons in yeast. We specifically focused on mutating N-terminal and C-terminal regions of the GFP protein so as not to affect its functional core. In addition, variants contained mostly synonymous mutations with two exceptions. We changed glutamic acids with aspartic acids at codon 5 and codon 234, and tyrosine with asparagine at codon 237 of the GFP gene. We created all constructs in three replicates, and estimated their noise through multiple independent experiments on different days.

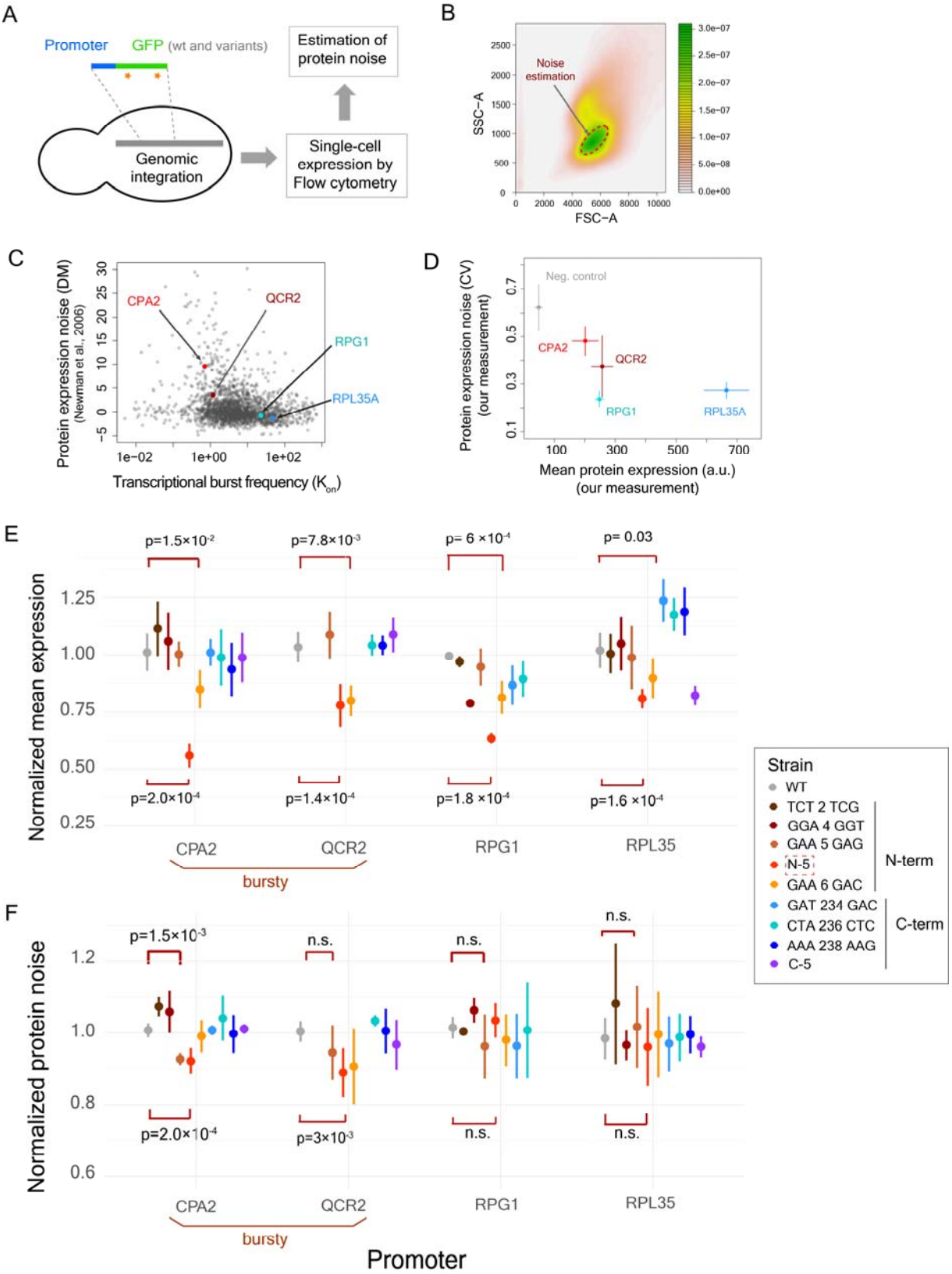

Fig. 5. Impact of changes in translational efficiency on protein noise is dependent on the transcriptional burst characteristics of promoters (A) Gene-promoter construct for genomic

integration and noise measurement **(B)** Noise estimation from a homogeneous group of cells with similar cell size and complexity **(C)** Protein noise (DM) vs burst frequency values for yeast genes **(D)** Measured protein noise of the promoters of *RPL35A*, *RPG1*, *CPA2* and *QCR2* in our constructs **(E-F)** Normalized mean protein expression (E) and normalized protein noise (F) of GFP variants under the regulation of the four promoters

The N-terminal single mutant variants contained TCT to TCG (S to S) mutation at codon 2, GGA to GGT (G to G) at codon 4, GAA to GAG (E to E) mutation at codon 5 and GAA to GAC (E to D) mutation at codon 6. The C-terminal single mutants contained GAT to GAC (D to D) mutation at codon 234, CTA to CTC (L to L) mutation at codon 236, and AAA to AAG (K to K) mutation at codon 238. The multi-mutant variant at the N-terminal end (denoted by N-5) contained five mutations, namely, TCT to TCG (S to S) at codon 2, AAA to AAG (K to K) at codon 3, GGA to GGT (G to G) at codon 4, GAA to GAG (E to E) at codon 5, and GAA to GAC (E to D) at codon 6. The multi-mutant variant at the C-terminal end (denoted by C-5) contained five mutations, namely, GAT to GAC (D to D) at codon 234, GAA to GAC (E to D) mutation at codon 235, CTA to CTC mutation (L to L) at codon 236, TAC to AAC mutation (Y to N) at codon 237, and AAA to AAG mutation (K to K) at codon 238.

The multi-mutant variant at the N-terminal end, containing five mutations (N-5), had the most number of rare codons and thus, was expected to show substantial reduction in mean protein expression owing to its low translational efficiency. We compared the impact of the coding region mutations across different promoters through the measures of normalized mean expression and normalized protein noise (Fig. 5E), to account for differences in mean protein expression and protein noise among the four promoters. The N-terminal multi-mutant (N-5) showed substantial reduction in normalized mean protein expression (~56-81% mean expression compared to the wild-type GFP gene) across all promoters. Very interestingly, the N-5 mutant

also showed substantial reduction in protein noise values, but only when expressed under the bursty promoters *CPA2* and *QCR2* (Fig. 5F). This mutant showed 8% and 11 % reduction in normalized protein noise compared to the wild-type GFP gene when expressed under the *CPA2* and *QCR2* promoters respectively (Mann-Whitney U test, $p=1.2\times10^{-4}$ and $p=6.7\times10^{-4}$ respectively), but showed much lower change in normalized protein noise when expressed under the regulation of the promoters *RPG1* and *RPL35A* (~3% increase and ~4% decrease in CV respectively) (Fig. 5F), despite 36% and 19% decrease in mean expression under the regulation of these non-bursty promoters.

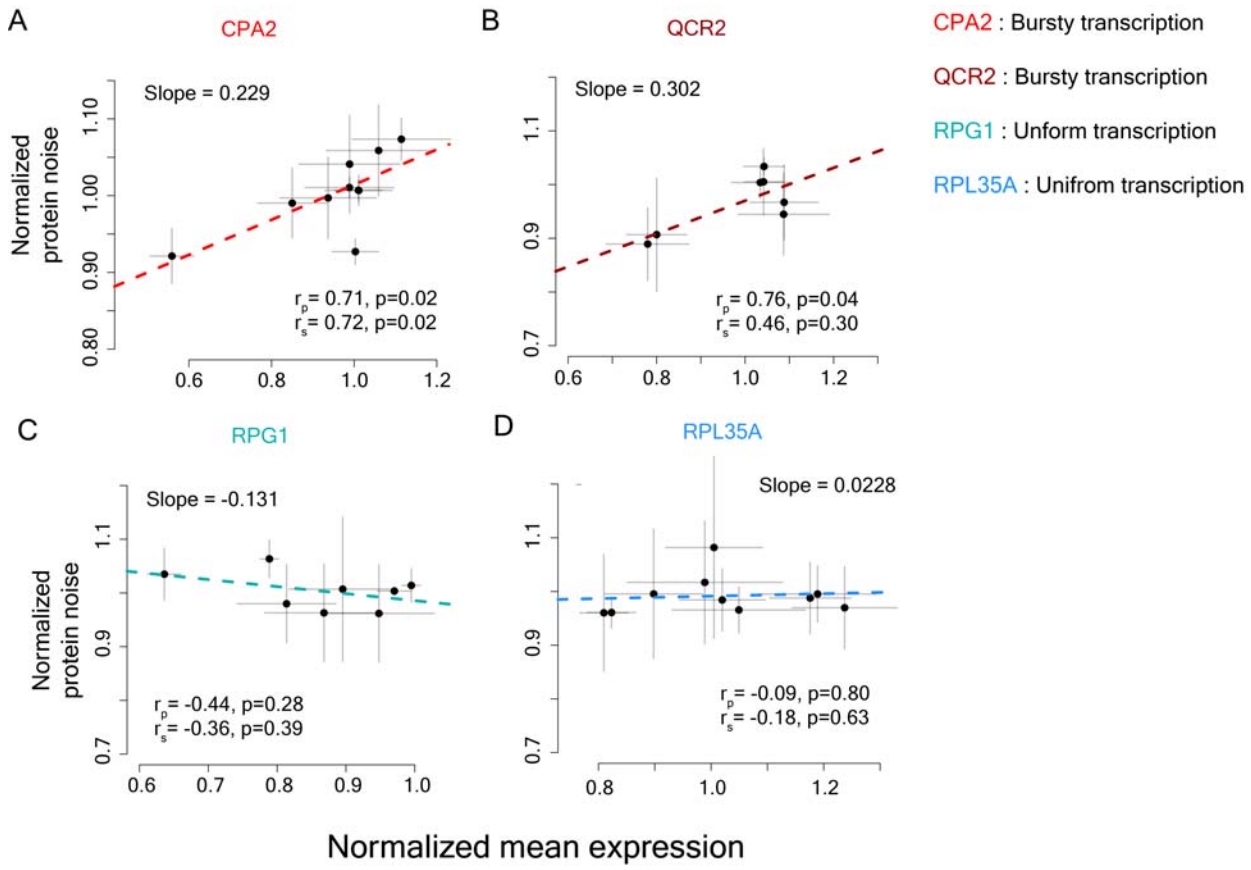

Figure 6 - Relationship between normalized protein noise and normalized mean expression across the four promoters – CPA2 (A), QCR2 (B), RPG1 (C) and RPL35A (D). CPA2 and QCR2 promoters show bursty transcription, whereas RPG1 and RPL35A show more uniform transcription.

Analysis of relationship between normalized protein noise and normalized mean expression across all GFP variants revealed very interesting results. The regression line fitted to the plot of normalized mean protein expression against normalized protein noise showed positive slopes only for bursty promoters CPA2 and QCR2 (slope of 0.229 and 0.302 respectively, Fig. 6A,B), like what had been observed before[30,31]. In contrast, the regression line for the promoters RPL35A and RPG1 showed near-zero or negative slope (Slope of -0.131 and 0.0228, respectively, Fig. 6C,D). Genome-wide analysis of relationship between protein noise and protein synthesis rate per mRNA or tAI for groups of genes with different transcriptional burst frequencies also showed similar trend, with stronger positive relationship between protein noise and translational efficiency for genes with bursty transcription ($K_{on} \leq Q_1$, first quartile of burst frequency) (Fig. S20). These results were in line with the predictions from stochastic simulations, and therefore, suggested that variation in ribosome demand was indeed the molecular link between stochastic fluctuations in mRNA numbers and protein noise.

Discussion

Taken together, our work provides unique molecular insights into the long-standing observation of positive correlation between translational efficiency and protein noise. We test the long-held assumption that low transcription rate combined with high translational efficiency can generate this positive correlation. We show that the high protein noise in genes with low transcription rate and high translational efficiency primarily stems from higher stochastic variation in mRNA numbers associated with low rate of transcription. We also show that demand for ribosomal machinery underlies translational modulation of transcriptional noise. Thus, our work reveals how the coding sequences of genes can influence expression noise, and how this contribution is

dependent on the properties of the promoter. This work also highlights how dynamic properties of a system and shared resources influence gene expression, beyond genetic features such as promoter sequence or presence of specific motifs.

Our results also illustrate how the translation process can decouple mean protein expression and protein noise[27], with a departure from the traditional inverse relationship between them. The nature and extent of translational decoupling is dictated by the translational efficiency of the coding sequence, as well as by the promoter and its mode of transcription.

There are several other factors besides codon usage that can impact translational efficiency. For example, presence of micro-ORF upstream of the start codon and presence of mRNA secondary structures in the 5' UTR region can affect translational efficiency [35,65]. In addition, presence of a stretch of positively- charged residues in the amino acid chain can slow down movement of the growing peptide chain through the ribosomal exit tunnel and can impact translational efficiency [66]. Thus, the effective translational efficiency for a gene is a complex combination of multiple variables. It remains to be seen how these variables combine with translational bursts and impact expression noise.

In summary, our work identifies variation in ribosome availability as the key feature driving the translational modulation of transcriptional bursts. Such variation happens across organisms and therefore, these results have broad implications for studying protein noise across biological systems. Advancements in single-cell RNA sequencing have enabled us to study mRNA expression noise across diverse cellular processes in different organisms. However, noise at the protein level has more direct impact on cellular phenotypes and therefore, on phenotypic

heterogeneity. Thus, a better understanding of how mRNA noise is linked to protein noise will help us better predict phenotypic heterogeneity. Our work further shows that combining estimates of burst parameters from single-cell RNA-sequencing data with tAI values of genes can help predict protein expression noise. As more single-cell RNA-seq data become available, this will greatly facilitate estimation of protein expression noise, and will enhance our understanding of its impact on cellular processes across different biological systems.

Materials and Methods

Datasets

The mean mRNA expression levels of yeast genes were calculated from the single-cell RNA-seq data in yeast[40]. Mean mRNA expression values for 5500 genes were obtained from this data. Noise in mRNA expression was calculated following the method described in Parab *et al.*[28]. Briefly, for each gene, mean expression, standard deviation and subsequently, coefficient of variation (CV) values were calculated. In the next step, polynomial functions of different degrees were fitted to the CV vs log-transformed mean mRNA expression plot, and the best fit was chosen. The polynomial function of order 5 was observed to give the best fit and was used for calculating mean-adjusted mRNA expression noise. For each gene, mean-adjusted mRNA noise was calculated by the distance of the vertical line drawn from its CV value to the fitted spline. Protein expression noise values for genes were obtained from Newman *et al.*[15] and their Distance-to-Median (DM) values, that were corrected for dependence of CV on mean protein expression, in YPD medium were used. Protein noise of 2763 genes were obtained from this data. For translational efficiency, the data from Riba *et al.*[41] were used, and for each gene, the real protein synthesis rate per mRNA value from their data was considered as its measure of

translational efficiency. The tAI values for all yeast genes were calculated using tAI value of each codon in yeast from Sabi *et al.*[67], according to the method described in Tuller *et al.*[34].

Two-state model for bursty transcription

Transcriptional bursts were modeled using a two-state model where a gene transitioned between on- and off- states[42]. The rate of transitions to on- and off- states were considered to follow Poisson distributions individually and thus, the time intervals between two on-transitions or off-transitions were exponentially distributed. The time intervals between successive events (on- or off- switching) were sampled from exponential distributions with rate parameters K_{on} and K_{off} respectively. Transitions to on-state resulted in production of mRNA at a rate β_m and translation of these mRNA molecules to proteins at a rate β_p. These mRNA and protein molecules were considered to undergo removal, resulting from dilution due to cell growth and degradation, at the rates of α_m and α_p respectively.

The dynamics of transcription and translation were modeled using the following equations.

$Change\ in\ mRNA\ conc.\ over\ time$: $\frac{d[mRNA]}{dt} = \beta_m - \alpha_m \times [\text{mRNA}]$ …… (Eq. 1)

where β_m denoted the transcription rate per unit time (or burst size) and α_m denoted the removal rate of mRNA due to degradation and dilution.

Similarly, $Change\ in\ protein\ conc.\ over\ time$: $\frac{d[P]}{dt} = \beta_p \times [\text{mRNA}] - \alpha_p[\text{P}]$ …… (Eq. 2)

where β_p denoted the protein production rate from mRNA and α_p denoted the protein removal rate.

Stochastic simulations were performed using Gillespie's algorithm[43] to model changes in the numbers of mRNA and protein molecules over time. The behavior of the system was tracked at small discrete time intervals Δt from the initial time point t. These resulted in observations at 'n+1' time points t, t+ Δt, t+2×Δt, …, t+n×Δt. Any event of binding or unbinding occurring within a time interval was noted and resulted in changes in transcription rate which eventually led to a change in protein concentration. As the time interval Δt was small, the equations modeling the behavior of the systems was simplified as

$$[mRNA]_{t+\Delta t} = [mRNA]_t+(\beta_m - \alpha_m\times[mRNA]_t)\times\Delta t \quad \text{…… (Eq. 3)}$$

and

$$[P]_{t+\Delta t} = [P]_t+(\beta_p\times[mRNA]_t - \alpha_p\times[P]_t)\times\Delta t \quad \text{……..(Eq. 4)}$$

β_m , α_m , β_p and α_p were expressed in appropriate units for further simplification of these equations. The base parameter values for the model were set as: K_{on} = 0.02, K_{off} = 0.2, β_m = 10 per unit time, β_p = 100 per mRNA molecule per unit time, α_m = 0.07 per mRNA molecule per unit time, and α_p = 0.007 per mRNA molecule per unit time. The dynamics of transcription, variation in the mRNA concentration and variation in protein concentration with time were modeled across 10,000 cells. Noise was expressed as coefficient of variation (CV) from the calculation of mean and standard deviation in the protein level across these 10,000 cells across all time points.

To investigate how the mean mRNA expression level and the transcriptional burst frequencies combine with translation rate (β_p) and impact protein noise, simulations were performed over a wide range of values of the parameters K_{on} and β_m. The parameter K_{on} was varied between 0.001 and 10, and the parameter β_m was varied between 1 to 1000 per unit time. For each value of these parameters, translation rate β_p was varied between a range of 1 to 1000 per mRNA molecule per unit time.

Estimation of burst parameters from single-cell RNA-seq data

The two-state model of gene expression enabled estimation of the parameters of transcriptional bursts from single-cell RNA-sequencing data using a maximum likelihood approach, as described by Kim and Marioni [44].

Specifically,

$$p \mid K_{on}, K_{off} \sim \text{Beta}\,(K_{on}, K_{off}) \quad \ldots\ldots\ldots\ldots\ldots \text{(Eq. 5)}$$

$$x \mid \beta_m, p \sim \text{Poisson}\,(\beta_m \cdot p) \quad \ldots\ldots\ldots\ldots\ldots \text{(Eq. 6)}$$

where 'x' is the number of RNA transcripts of a given gene within a cell and 'p' is an auxiliary variable following a beta distribution. The mean of the parameter 'p' is equal to the fraction of time that a gene spends in the active state. The resultant marginal distribution is known as Poisson-Beta distribution, denoted by $P\,(x \mid K_{on}, K_{off}, \beta_m)$, and gives the steady-state distribution for the mRNA copy numbers across cells. All parameters are further normalized by α_m. K_{on} and K_{off} control the shape of the Beta distribution and represent the probability of a gene being in 'on' and 'off' states, respectively. β_m is the mean of Poisson distribution and represents the average rate of gene expression when the gene is in the 'on' state.

The yeast single cell RNA-seq data[40] was given as the input to the model. The two-state model parameters $\theta = (K_{on}, K_{off}, \beta_m)$ were inferred by maximizing the likelihood of the parameters of Poisson-Beta distribution for a given set of observed data points X. This can be represented as:

$$arg_{max(\theta\ in\ \Theta)} = \prod_{\{x\ in\ X\}} P(x|\theta) \quad \ldots\ldots \text{(Eq. 7)}$$

This was further represented as maximization of the log-likelihood, which was equivalent to minimization of the negative log-likelihood:

$$arg_{max(\theta\ in\ \Theta)} = \sum_{\{x\ in\ X\}} \ln(P(x|\theta)) \qquad \text{……. (Eq. 8)}$$

$$arg_{min(\theta\ in\ \Theta)} = -\sum_{\{x\ in\ X\}} \ln(P(x|\theta)) \qquad \text{…….. (Eq. 9)}$$

The negative log-likelihood was minimized using L-BFGS-B approach[68] and the resulting distributions for parameters in θ were calculated.

Mathematical model of translation at single mRNA level for capturing bursty translation

Several mathematical models for the translation process have been described, and they include the TASEP model, the Ribosome Flow Model (RFM) and their variants[45,46,69-72]. Totally Asymmetric Simple Exclusion Process or TASEP model assumes that an mRNA molecule is a one-dimensional lattice through which a ribosome can hop in only one direction from one site to the next, provided the latter is empty.

To capture the dynamics of translation, a simple TASEP-based model with appropriate modifications was developed and bursty translation was incorporated. To start with, translational bursts were assumed to arise due to stochastic transitions of an mRNA molecule between active and inactive states with the rates TL_{on} and TL_{off} respectively. In the active state, translation initiation on the mRNA molecule occurred at a rate TL_{init}. The parameters TL_{on} and TL_{off} were assumed to follow Poisson distributions individually and hence, the time-intervals between two subsequent on-states (or off-states) were assumed to follow exponential distributions. The parameter values were chosen within the range of parameter values observed or estimated from experimental datasets, to build a realistic model. For yeast genes, maximum likelihood estimates of K_{on} and K_{off} from single-cell RNA-seq data[40] were in the ranges of 0.005 to 744, and 0.001 to 1000, respectively. In yeast, the experimental estimates for mRNA synthesis rates ranged from

~0.01 to 4 per min[73], and protein synthesis rates per mRNA ranged from 0-13.6 per sec per mRNA [41]. Earlier Estimates for mRNA half-life ranged from 3 mins to 300 mins[74] but a recent non-invasive measurement of mRNA half-life has found that majority of mRNA molecules in yeast have half-lives of less than 10 mins[64]. The estimates for protein half-life ranged from 2 mins to ~16000 mins[75]. However, no estimates for TL_{on} and TL_{off} were available. Large values of K_{on}, TL_{on}, mRNA synthesis rate, protein synthesis rates, mRNA half-life and protein half-life made simulations extremely slow and computationally very demanding, as the model had to track many mRNA molecules and translation initiation events. Therefore, these values were not explored. In addition, genes with very stable mRNA molecules are unlikely to show fluctuation in mRNA numbers and therefore, are not of interest to this study.

As multiple ribosomes could translate a single mRNA molecule at the same time, a second translation initiation happened only when the earlier mRNA bound ribosome had moved by 10 or more codons on the mRNA molecule, thus, accounting for steric interactions between two ribosomes[47,48]. Movement of ribosome through an mRNA molecule depends on the individual codons that are present. Preferred codons for which tRNA molecules are readily available are traversed quickly, whereas the rare codons are read slower. Tuller *et al.*[34] observed a specific and conserved translational profile across several species where translational efficiency was low at the start of the genes for about 30-50 codons, followed by a gradual increase to the maximum efficiency. Similarly, Weinberg *et al.*[49] observed a slow rate of translation, although to a different degree, in the first 200 nucleotides of a gene. This enabled us to model ribosome traversal speed in a more general manner rather than focusing on the occurrence of specific codons that would vary from one gene to another. The ribosome traversal speed was modeled using a first order Hill function of the following form

$$V = \frac{V_{max}L}{K_{Hill}+L} \quad \text{..... (Eq. 10)}$$

Where, V = traversal speed of the ribosome at codon L in the mRNA molecule, V_{max} = maximum traversal speed of the ribosome in the mRNA molecule, K_{Hill} = constant, and L = position in the mRNA. The values of V_{max} and K_{Hill} were chosen to be 100 codons per min and 30 respectively. All parameters were further varied and tested for model robustness as discussed below.

The value of K_{Hill} influenced the relationship between the traversal speed and the position L, and eventually determined the time taken for a ribosome to completely traverse through a mRNA molecule. High values of K_{Hill} reduced the number of translation initiation events, thus mimicking the scenario of lower translational efficiency. This is because a ribosome took longer time to traverse through the first 10 codons, which was required before the next translation initiation event could take place. A reduction in the value of K_{Hill} allowed higher translation initiation rate (TL_{init}) and captured the behavior of the system in case of high translational efficiency. Conversely, increasing the translation initiation rate required the K_{Hill} value to be lower. Thus, the relationship between K_{Hill} and translation initiation rate (TL_{init}) was modeled using the equation

$$K_{Hill} = A \times (1 + \frac{B}{B + \mathrm{TL}_{init}}) \quad \text{..... (Eq. 11)}$$

Where A and B were constants. The values of A and B shaped the relationship between K_{Hill} and β_p, and in our model were chosen as 20 and 5 respectively. Higher translational efficiency led to faster traversal of ribosome through an mRNA molecule and allowed more translation initiation events leading to higher value of β_p. The model was tested with different values of the parameters K_{Hill}, A, B and V_{max} to test for robustness.

In the next step, the model of translation at the single mRNA level was integrated with the two-state model of transcription, and the combined model was utilized for subsequent stochastic simulations. The base parameter values for the model were chosen as: K_{on} = 0.02, K_{off} = 0.2, β_m = 4 per minute, TL_{on}=0.5, TL_{off}=0.5, A=20, B=5, K_{Hill}=30, V_{max}=100 codons per minute, Length of the gene (L_{tot}) = 300 codons, mRNA half-life (HL_{mRNA}) = 10 mins, and protein half-life (HL_{prot}) = 100 mins.

Every mRNA molecule generated through transcriptional burst was tracked by the translation model at every minute over the life-time of the mRNA molecule, and the protein expression at every time-point was estimated. Gillespie's algorithm was used for simulations in 1000 cells through which estimates for population-wide mean protein expression and protein noise were derived. The process was repeated for a wide-range of transcriptional and translational burst frequency values, as well as for other parameters of the models, to investigate whether positive correlation between mean protein expression and protein noise could be observed at specific parameter values. The K_{on} parameter was varied between 0.01 and 10, the K_{off} parameter was varied between 0.01 and 10, TL_{on} between 0.01 and 5, TL_{off} between 0.01 and 5, and β_m between 0.1 to 20 per min. For each of these parameter values, TL_{init} was varied between 0.1 and 10 per mRNA molecule per minute. The values of mRNA and protein half-lives were stochastically varied by ±10% of the chosen value, as the half-lives of individual mRNA and protein molecules can vary within a cell.

Modeling and simulation of demand for ribosomal machinery

As multiple mRNA molecules share a common pool of ribosomal machinery for translation, the number of ribosomes available for translating a specific mRNA molecule can vary with time. Several studies have modeled the translation process with finite resources and competition, however, none of them had investigated the impact on protein expression levels or on heterogeneity. Only one earlier study, investing the stochastic nature of translation using mathematical models, predicted that use of rare codons will increase expression heterogeneity[76], which contradicted the empirical observations.

Competition for a finite pool of ribosomal machinery would impact the translation initiation rate in an mRNA molecule. High availability of ribosomal machinery would lead to high translation initiation rate, whereas a scarcity of ribosomes would lower translation initiation rate. Transcriptional bursts generate stochastic fluctuations in mRNA numbers over time which can lead to a variable demand for ribosomal machinery required for translation. When the number of mRNA molecules of a gene increases suddenly due to a transcriptional burst, the demand for ribosomal machinery increases rapidly. Subsequently, when the mRNA numbers fall, this lowers demand and frees up ribosomes, which can then be utilized for translating mRNA molecules of other genes.

The demand for ribosomal machinery was incorporated in the model of translation so that its effect on translation initiation rate of an mRNA molecule could be captured. For a gene, the number of mRNA molecules produced by transcriptional burst and the number of ribosomes bound to mRNA molecules were tracked at every time point. At every time point, the ribosome demand was modeled using different functions that incorporated the ratio of current mRNA numbers to the mRNA numbers at the previous time point, the ratio of current number of bound

ribosomes to the number of bound ribosomes at the previous time point or a combination of both (Table S1). These included functions where the translation initiation rate at a specific time point was equal to the base translation initiation rate divided by the ribosome demand, or more complex Hill functions of order 10 (Table S1), that could induce sharp transitions in translation initiation rate when demand was too high. Higher number of mRNA molecules or ribosomes bound to mRNA at a time point compared to the previous time point meant lower availability of ribosomal machinery for translation and lower translation initiation rate. Among all functions tested, the one which considered both number of mRNA molecules and number of bound ribosomes at current and previous time points, and modeled the impact of ribosome availability on translation initiation rate through Hill function (Function 14 to Function 19, Table S1) generated the best positive correlation between mean protein expression and protein noise (Fig. S8). The function 16 was used for all subsequent analysis.

The integrated model of bursty transcription and bursty translation incorporating ribosome demand was tested in a wide range of values of several parameters. The impact of variation in values of the parameters K_{Hill}, A, B and maximum ribosome traversal rate (V_{max}) individually on correlation between protein noise and translational efficiency was tested. The parameter K_{Hill} was varied between 20 and 60, A between 10 and 50, B between 1 and 10, V_{max} between 50 and 150. For each of the parameter values, the translation initiation rate (TL_{init}) was varied between 0.1 and 10 per mRNA molecule per min. For $V_{max} = 50$, no protein expression was observed. For the rest of the parameter values, no effect on correlation between translational efficiency and protein noise was observed (Fig. S9-S12).

In the next step, the model was tested with different values of the parameters K_{on}, K_{off}, TL_{on}, TL_{off}, and β_m. Each of these parameters was varied individually and the impact of changes in the translation initiation rate (TL_{init}) on protein noise was tested (Fig. 4D,E; Fig. S13-S15). The parameter K_{on} was varied between 0.01 and 10, K_{off} between 0.01 and 10, TL_{on} between 0.01 and 5, TL_{off} between 0.01 and 5, and β_m between 0.1 and 20. For each of these parameter values, TL_{init} was varied between 0.1 and 10 per mRNA molecule per min. Higher rates of β_m and TL_{init} made simulations extremely slow and computationally very demanding, as the model had to track a large number of mRNA molecules and translation initiation events, respectively. Therefore, these values could not be used for simulation.

Since it was not possible to explore all possible combinations of parameter values due to an extremely large number of combinations, random sampling of parameter values for K_{on}, K_{off}, TL_{on}, TL_{off}, β_m, HL_{mRNA} and $HL_{protein}$ were performed from a specified range of each parameter (Fig. S16). This also enabled us to study how different combinations of values of these parameters impact protein noise, and consequently, the relationship between translational efficiency and protein noise. Fifty random sampling of parameter values were done and for each set of parameter values, the translation rate (β_p) was varied between 0.2 and 10 per mRNA molecule per min. The parameter K_{on} was sampled in the range of 0.01 to 2, K_{off} between 0.01 and 2, TL_{on} between 0.1 and 5, β_m between 0.1 and 10 per min, HL_{mRNA} between 1 and 20 mins, and HL_{prot} between 1 and 200 mins. Simulation results indicated interactions between different parameter values that also impacted the relationship between translational efficiency and protein noise (Fig. S16).

Construction of GFP-promoter fragment and genomic integration in yeast

Saccharomyces cerevisiae BY4741 strain was used for experiments. *Green Fluorescent Protein* (*GFP*) gene integrated in the yeast genome was used as the model system for noise quantification. The gene-promoter construct was made as follows. The *GFP* gene was amplified from the yeast strain where the *PDR5* gene was tagged with *GFP*, and the first two codons ATG and TCT were added with the help of primers (Table S2). For PCR amplification, genomic DNA from yeast was isolated by lithium acetate-SDS method and 2 µl genomic DNA was used as template. Amplification using Q5 DNA polymerase and gene-specific primers was performed, and the PCR product subsequently purified using QIA quick PCR Purification Kit (Qiagen).

The strain BY4741 has a truncated and non-functional *HIS3* gene (*his3Δ1*). Therefore, the gene-promoter construct was inserted into the site of the *HIS3* gene through homologous recombination, and *HIS3MX6* cassette was used as the auxotrophic marker for selection of transformed colonies. The *HIS3MX6* cassette was amplified from yeast strain with *PDR5-GFP* fusion. For genomic integration, the genomic regions upstream and downstream region of the *HIS3* gene, denoted by His3L and His3R respectively (Fig. S17), were amplified and were separately cloned into pUC19 vector with restriction digestion and ligation. The constructs were transformed into chemically competent *E. coli* cells[77] and the transformed bacterial colonies were selected on LB plates supplemented with 100 µg/ml ampicillin. The promoters, the *GFP* gene and the *HIS3MX6* cassette were subsequently cloned step-by-step through restriction digestion with appropriate enzymes (Fig. S17), followed by ligation with T4 DNA ligase. The constructs were transformed into *E. coli* and were selected on LB plates supplemented with ampicillin. The cloned DNA fragments were verified by restriction digestion of the constructed fragment, as well as through Sanger sequencing. Promoters of four genes, namely, *RPG1*, *RPL35A*, *CPA2* and *QCR2* were cloned upstream of the *GFP* gene (Table S3). The genes *CPA2*

and *QCR2* showed high protein noise and the genes *RPG1* and *RPL35A* showed low protein noise in genome-wide noise data of yeast[15]. For cloning promoter sequence of a gene, the region between the start codon of the gene and the stop codon of the previous gene on the same DNA strand was considered (Table S3).

In the next step, the full construct was amplified using His3L forward and His3R reverse primers (Table S2) using Q5 polymerase, and 20 µl of the PCR product was used for transformation into competent yeast cells following the protocol of Gietz and Schiestl[78]. Briefly, yeast cells were first grown to saturation in YPD medium at 30°C overnight, and then were diluted into fresh medium, where they were allowed to grow for 4 hours. Cells were precipitated, and were washed once with 0.1M lithium acetate (LiAc) solution. Cells were resuspended in 50µl of 0.1M LiAc and then 5µl salmon sperm carrier DNA along with 20µl of PCR product were added. Further, 300 µl of PLI solution, comprising of 10% (v/v) 1M LiAC, 10% (v/v) water and 80% (v/v) PEG 3350 (50% w/v), was added to each tube. Cells were subjected to heat shock at 42°C for 40 minutes, following which PLI solution was removed, and the cells were plated on synthetic complete medium supplemented with 2% glucose but without any histidine (SD-His). Colonies with genomic integration were confirmed by colony PCR, and subsequently, were verified by Sanger sequencing.

Generation of single- and multi-mutant variants of GFP

Seven mutant variants of the *GFP* gene were constructed, out of which three variants contained mutations in the N-terminal region and four variants contained mutations in the C-terminal region. Variants with mutations in the N-terminal or C-terminal regions were targeted to prevent

disturbing the catalytic core of the GFP protein. The mutant variants were cloned downstream of the four promoters.

The N-terminal single mutant variants consisted of TCT to TCG (S to S) mutation at codon 2, GGA to GGT (G to G) mutation at codon 4, GAA to GAG (E to E) mutation at codon 5 and GAA to GAC (E to D) mutation at codon 6. The C-terminal single mutants consisted of GAT to GAC (D to D) mutation at codon 234, CTA to CTC (L to L) mutation at codon 236, and AAA to AAG (K to K) mutation at codon 238. The multi-mutant variant at the N-terminal end (denoted by N-5) contained five mutations, namely, TCT to TCG (S to S) at codon 2, AAA to AAG (K to K) at codon 3, GGA to GGT (G to G) at codon 4, GAA to GAG (E to E) at codon 5, and GAA to GAC (E to D) at codon 6. The multi-mutant variant at the C-terminal end (denoted by C-5) contained five mutations, namely, GAT to GAC (D to D) at codon 234, GAA to GAC (E to D) mutation at codon 235, CTA to CTC mutation (L to L) at codon 236, TAC to AAC mutation (Y to N) at codon 237, and AAA to AAG mutation (K to K) at codon 238.

To construct and clone the mutant variants of the GFP gene downstream of the promoter regions, an overlap extension PCR method following the protocol described in Higuchi *et al.*[79] was used. For generating the mutant variants, primers were designed keeping the target mutation at the center with 15 bases flanking them on each side. In the first amplification step, two fragments were generated. The first fragment was from the 5' end of Hi3L region till the targeted mutation site in the *GFP* gene, and the second fragment was from the targeted mutation site in the *GFP* gene till the 3' end region of His3R (Fig. S21). Amplification was carried out using high-fidelity Q5 DNA polymerase. The reaction mixture comprised of 2.5 µl of each primer (10 µM), 10 µl of 5x Q5 reaction buffer, 1 µl of 10 mM dNTPs, 0.5 µl of Q5 DNA polymerase (New England

Biolabs) and molecular biology grade water to a total volume of 50 µl. The PCR program consisted of incubation at 98 °C for 1 min (initial denaturation) followed by 30 cycles of 98°C for 10 sec (denaturation), 65°C for 30 sec (annealing), 72°C for 1 min 30 sec (extension), and a final extension at 72°C for 10 min.

The products after amplification were treated with 1 µl of ExoSAP-IT PCR product cleanup reagent (Thermo Fisher Scientific) and 0.5 µl DpnI (New England Biolabs) for 1 hr at 37°C, followed by deactivation for 20 min at 80 °C. The products were then purified using QIAquick PCR Purification Kit (Qiagen) and quantified using Qubit 4 Fluorometer (Thermo Fisher Scientific).

As the molecular weight of the amplified fragments were variable, equimolar concentration of the fragments from the previous amplification step were used in the next step. For each reaction, 0.5 to 1 picomole of each purified fragment were used as templates. For assembly, the reaction mixture comprised of equimolar content of two template fragments, 10 µl of 5x Q5 reaction buffer, 1 µl of 10 mM dNTPs, 0.5 µl of Q5 DNA polymerase (New England Biolabs) and molecular biology grade water to a total volume of 45 µl, without any primer. The program consisted of incubation at 98 °C for 1 min (initial denaturation) followed by 10 cycles of 98°C for 10 sec (denaturation), 60°C for 30 sec (annealing) and 72°C for 1 min 30 sec (extension). On completion of 10th cycle, 2.5 µl of forward and reverse primers (10 µM stock of each) were added, and the program was run for next 25 cycles by raising the annealing temperature to 72°C. The reaction was terminated by a final extension at 72°C for 10 min.

The assembled mutant constructs were then directly transformed into competent yeast cells following the LiAC method as described above, and the transformants were selected on SD-His plates. The clones were confirmed by colony PCR and Sanger sequencing.

Measurement of expression noise using flow cytometry

Three clones of wild-type GFP gene and each mutant variant were picked for noise measurement in flow cytometry. Yeast cultures were grown in SCD medium (0.67% YNB + 0.079% complete synthetic supplement + 2% glucose) at 30□ with shaking at 220 rpm. Yeast cells from glycerol stock were inoculated in SCD medium, were grown for 24 hours, and were then diluted 1:100 in fresh medium. This process was repeated one more time. The cells were then diluted 1:50 in fresh SCD and were grown for 4 hours. In the next step, cells were centrifuged and washed twice with 1X PBS (Phosphate Buffered Saline) buffer, and were finally resuspended in 1X PBS buffer for flow cytometry. In flow cytometry, the data were acquired for 2,00,000 cells for each sample in a BD LSR Fortessa cell analyzer (Fig. S18). To minimize heterogeneity in signal due to heterogeneity in cell size and complexity, a small homogeneous subset of cells with similar size and complexity parameters (FSC-A and SSC-A) were filtered. Ellipses with different lengths of major and minor axes were fitted to the FSC-A vs SSC-A plot, and the best fit that covered the most of homogeneous cells was chosen (Fig. S19). This also filtered out cell aggregates or budding cells which can have higher GFP signal than single cells. The data from these cells were then used for calculation of expression noise. The data were analyzed using custom R codes based on codes from Silander *et al.*[14]. Normalized mean expression and normalized noise value for a strain in an experiment was calculated by dividing the mean expression and noise values with the corresponding values for the wild-type variant in that experiment.

References

1. N. Q. Balaban, J. Merrin, R. Chait, L. Kowalik, S. Leibler, Bacterial persistence as a phenotypic switch. *Science* **305**, 1622-1625 (2004). doi: 10.1126/science.1099390.

2. Y. Wakamoto, N. Dhar, R. Chait, K. Schneider, F. Signorino-Gelo, S. Leibler, J. D. McKinney, Dynamic persistence of antibiotic-stressed mycobacteria. *Science* **339**, 91-95 (2013). doi: 10.1126/science.1229858.

3. A. Raj, S. A. Rifkin, E. Andersen, A. van Oudenaarden, Variability in gene expression underlies incomplete penetrance. *Nature* **463**, 913-918 (2010). doi: 10.1038/nature08781.

4. A. Burga, M. O. Casanueva, B. Lehner, Predicting mutation outcome from early stochastic variation in genetic interaction partners. *Nature* **480**, 250-253 (2011). doi: 10.1038/nature10665.

5. A. Eldar, V. K. Chary, P. Xenopoulos, M. E. Fontes, O. C. Losón, J. Dworkin, P. J. Piggot, M. B. Elowitz, Partial penetrance facilitates developmental evolution in bacteria. *Nature* **460**, 510-514 (2009). doi: 10.1038/nature08150.

6. Y. Lu, K. Bohn-Wippert, P. J. Pazerunas, J. M. Moy, H. Singh, R. D. Dar, Screening for gene expression fluctuations reveals latency-promoting agents of HIV. *Proc Natl Acad Sci USA* **118**, e2012191118 (2021). doi: 10.1073/pnas.2012191118.

7. M. A. Coomer, L. Ham, M. P. H. Stumpf, Noise distorts the epigenetic landscape and shapes cell-fate decisions. *Cell Syst.* **13**, 83-102.e6 (2022). doi: 10.1016/j.cels.2021.09.002.

8. A. Nguyen, M. Yoshida, H. Goodarzi, S. F. Tavazoie, Highly variable cancer subpopulations that exhibit enhanced transcriptome variability and metastatic fitness. *Nat Commun*. **7**, 11246 (2016). doi: 10.1038/ncomms11246.

9. A. Sharma, E. Merritt, X. Hu, A. Cruz, C. Jiang, H. Sarkodie, Z. Zhou, J. Malhotra, G. M. Riedlinger, S. De, Non-Genetic Intra-Tumor Heterogeneity Is a Major Predictor of Phenotypic Heterogeneity and Ongoing Evolutionary Dynamics in Lung Tumors. *Cell Rep*. **29**, 2164-2174.e5 (2019). doi: 10.1016/j.celrep.2019.10.045.

10. B. L. Emert, C. J. Cote, E. A. Torre, I. P. Dardani, C. L. Jiang, N. Jain, S. M. Shaffer, A. Raj, Variability within rare cell states enables multiple paths toward drug resistance. *Nat Biotechnol*. **39**, 865-876 (2021). doi: 10.1038/s41587-021-00837-3.

11. I. Golding, J. Paulsson, S. M. Zawilski, E. C. Cox, Real-time kinetics of gene activity in individual bacteria. *Cell* **123**,1025-1036 (2005). doi: 10.1016/j.cell.2005.09.031.

12. L. Cai, N. Friedman, X. S. Xie, Stochastic protein expression in individual cells at the single molecule level. *Nature* **440**, 358-62 (2006). doi: 10.1038/nature04599.

13. A. Raj, C. S. Peskin, D. Tranchina, D. Y. Vargas, S. Tyagi, Stochastic mRNA synthesis in mammalian cells. *PLoS Biol.* **4**, e309 (2006). doi: 10.1371/journal.pbio.0040309.

14. O. K. Silander, N. Nikolic, A. Zaslaver, A. Bren, I. Kikoin, U. Alon, M. Ackermann, A genome-wide analysis of promoter-mediated phenotypic noise in *Escherichia coli*. *PLoS Genet.* **8**, e1002443 (2012). doi: 10.1371/journal.pgen.1002443.

15. J. R. Newman, S. Ghaemmaghami, J. Ihmels, D. K. Breslow, M. Noble, J. L. DeRisi, J. S. Weissman, Single-cell proteomic analysis of *S. cerevisiae* reveals the architecture of biological noise. *Nature*, **441,** 840-846 (2006). doi: 10.1038/nature04785.

16. A. Bar-Even, J. Paulsson, N. Maheshri, M. Carmi, E. O'Shea, Y. Pilpel, N. Barkai, Noise in protein expression scales with natural protein abundance. *Nat Genet.* **38,** 636-643 (2006). doi: 10.1038/ng1807.

17. D. M. Suter, N. Molina, D. Gatfield, K. Schneider, U. Schibler, F. Naef, Mammalian genes are transcribed with widely different bursting kinetics. *Science* **332**, 472-4 (2011). doi: 10.1126/science.1198817.

18. R. D. Dar, B. S. Razooky, A. Singh, T. V. Trimeloni, J. M. McCollum, C. D. Cox, M. L. Simpson, L. S. Weinberger, Transcriptional burst frequency and burst size are equally modulated across the human genome. *Proc Natl Acad Sci USA* **109**, 17454-17459 (2012). doi: 10.1073/pnas.1213530109

19. I. Tirosh, A. Weinberger, M. Carmi, N. Barkai, A genetic signature of interspecies variations in gene expression. *Nat Genet.* **38**, 830-834 (2006). doi: 10.1038/ng1819.

20. J. M. Raser, E. K. O'Shea, Control of stochasticity in eukaryotic gene expression. *Science* **304**, 1811-1814 (2004). doi: 10.1126/science.1098641.

21. C. N. Ravarani, G. Chalancon, M. Breker, N. S. de Groot, M. M. Babu, Affinity and competition for TBP are molecular determinants of gene expression noise. *Nat Commun*. **7,** 10417 (2016). doi: 10.1038/ncomms10417.

22. I. Tirosh, N. Barkai, Two strategies for gene regulation by promoter nucleosomes. *Genome Res.* **18**, 1084-1091 (2008). doi: 10.1101/gr.076059.108.

23. J. K. Choi, Y. J. Kim, Intrinsic variability of gene expression encoded in nucleosome positioning sequences. *Nat Genet*. **41**, 498-503 (2009). doi: 10.1038/ng.319.

24. X. Chen, J. Zhang, The Genomic Landscape of Position Effects on Protein Expression Level and Noise in Yeast. *Cell Syst.* **2**, 347-354 (2016). doi: 10.1016/j.cels.2016.03.009.

25. A. J. Faure, J. M. Schmiedel, B. Lehner, Systematic Analysis of the Determinants of Gene Expression Noise in Embryonic Stem Cells. *Cell Syst.* **5**, 471-484.e4 (2017). doi: 10.1016/j.cels.2017.10.003.

26. B. T. Donovan, A. Huynh, D. A. Ball, H. P. Patel, M. G. Poirier, D. R. Larson, M. L. Ferguson, T. L. Lenstra. Live-cell imaging reveals the interplay between transcription factors, nucleosomes, and bursting. *EMBO J*. **38**, e100809 (2019). doi: 10.15252/embj.2018100809.

27. K. Loell, Y. Wu, M. V. Staller, B. Cohen, Activation domains can decouple the mean and noise of gene expression. *Cell Rep.* **40**, 111118 (2022). doi: 10.1016/j.celrep.2022.111118.

28. L. Parab, S. Pal, R. Dhar, Transcription factor binding process is the primary driver of noise in gene expression. *PLoS Genet.* **18**, e1010535 (2022). doi: 10.1371/journal.pgen.1010535.

29. Y. Taniguchi, P. J. Choi, G. W. Li, H. Chen, M. Babu, J. Hearn, A. Emili, X. S. Xie, Quantifying *E. coli* proteome and transcriptome with single-molecule sensitivity in single cells. *Science* **329**, 533-538 (2010). doi: 10.1126/science.1188308.

30. E. M. Ozbudak, M. Thattai, I. Kurtser, A. D. Grossman, A. van Oudenaarden, Regulation of noise in the expression of a single gene. *Nat Genet.* **31**, 69-73 (2002). doi: 10.1038/ng869.

31. W. J. Blake, M. Kaern, C. R. Cantor, J. J. Collins, Noise in eukaryotic gene expression. *Nature* 422, 633-637 (2003). doi: 10.1038/nature01546.

32. R. Salari, D. Wojtowicz, J. Zheng, D. Levens, Y. Pilpel, T. M. Przytycka, Teasing apart translational and transcriptional components of stochastic variations in eukaryotic gene expression. *PLoS Comput Biol.* **8**, e1002644 (2012). doi: 10.1371/journal.pcbi.1002644.

33 M. dos Reis, R. Savva, L. Wernisch, Solving the riddle of codon usage preferences: a test for translational selection. *Nucleic Acids Res.* 32, 5036-44 (2004). doi: 10.1093/nar/gkh834.

34. T. Tuller, A. Carmi, K. Vestsigian, S. Navon, Y. Dorfan, J. Zaborske, T. Pan, O. Dahan, I. Furman, Y. Pilpel, An evolutionarily conserved mechanism for controlling the efficiency of protein translation. *Cell* **141,** 344-354 (2010). doi: 10.1016/j.cell.2010.03.031.

35. H. W. Wu, E. Fajiculay, J. F. Wu, C. S. Yan, C. P. Hsu, S. H. Wu, Noise reduction by upstream open reading frames. *Nat Plants*. **8,** 474-480 (2022). doi: 10.1038/s41477-022-01136-8.

36. H. B. Fraser, A. E. Hirsh, G. Giaever, J. Kumm, M. B. Eisen, Noise minimization in eukaryotic gene expression. *PLoS Biol*. **2**, e137 (2004). doi: 10.1371/journal.pbio.0020137.

37. Y. Pilpel, "Noise in biological systems: pros, cons, and mechanisms of control" in *Yeast Systems Biology* (Humana Press, 2011) pp. 407-25. doi: 10.1007/978-1-61779-173-4_23.

38. B. Wu, C. Eliscovich, Y. J. Yoon, R. H. Singer, Translation dynamics of single mRNAs in live cells and neurons. *Science* **352**, 1430-1435 (2016). doi: 10.1126/science.aaf1084.

39. N. M. Livingston, J. Kwon, O. Valera, J. A. Saba, N. K. Sinha, P. Reddy, B. Nelson, C. Wolfe, T. Ha, R. Green, J. Liu, B. Wu, Bursting translation on single mRNAs in live cells. *Mol Cell*. **83**, 2276-2289.e11 (2023). doi: 10.1016/j.molcel.2023.05.019.

40. M. Nadal-Ribelles, S. Islam, W. Wei, P. Latorre, M. Nguyen, E. de Nadal, F. Posas, L. M. Steinmetz, Sensitive high-throughput single-cell RNA-seq reveals within-clonal transcript

correlations in yeast populations. *Nat Microbiol*. **4**, 683-692 (2019). doi: 10.1038/s41564-018-0346-9.

41. A. Riba, N. Di Nanni, N. Mittal, E. Arhné, A. Schmidt, M. Zavolan, Protein synthesis rates and ribosome occupancies reveal determinants of translation elongation rates. *Proc Natl Acad Sci USA* **116**:15023-15032 (2019). doi: 10.1073/pnas.1817299116.

42. J. Peccoud, B. Ycart, Markovian modeling of gene-product synthesis. *Theor. Popul. Biol*. **48**, 222-234 (1995).

43. D. T. Gillespie, Exact stochastic simulation of coupled chemical reactions. *J. Phys. Chem.* **81**, 2340–2361 (1977).

44. J. K. Kim, J. C. Marioni, Inferring the kinetics of stochastic gene expression from single-cell RNA-sequencing data. *Genome Biol.* **14**, R7 (2013). doi: 10.1186/gb-2013-14-1-r7.

45. R.K.P. Zia, J. J. Dong, B. Schmittmann, Modeling Translation in Protein Synthesis with TASEP: A Tutorial and Recent Developments. *J Stat Phys* **144**, 405–428 (2011).

46. D. E. Andreev, M. Arnold, S. J. Kiniry, G. Loughran, A. M. Michel, D. Rachinskii, P. V. Baranov, TASEP modelling provides a parsimonious explanation for the ability of a single uORF to derepress translation during the integrated stress response. *Elife* **7,** e32563 (2018). doi: 10.7554/eLife.32563.

47. J. A. Steitz, Polypeptide chain initiation: nucleotide sequences of the three ribosomal binding sites in bacteriophage R17 RNA. *Nature* **224,** 957-964 (1969). doi: 10.1038/224957a0.

48. N. T. Ingolia, S. Ghaemmaghami, J. R. Newman, J. S. Weissman, Genome-wide analysis in vivo of translation with nucleotide resolution using ribosome profiling. *Science* **324**, 218-223 (2009). doi: 10.1126/science.1168978.

49. D. E. Weinberg, P. Shah, S. W. Eichhorn, J. A. Hussmann, J. B. Plotkin, D. P. Bartel. Improved Ribosome-Footprint and mRNA Measurements Provide Insights into Dynamics and Regulation of Yeast Translation. *Cell Rep.* **14**, 1787-1799 (2016). doi: 10.1016/j.celrep.2016.01.043.

50. C. L. Barrington, G. Galindo, A. L. Koch, E. R. Horton, E. J. Morrison, S. Tisa, T. J. Stasevich, O. S. Rissland. Synonymous codon usage regulates translation initiation. *Cell Rep.* **42**, 113413 (2023). doi: 10.1016/j.celrep.2023.113413.

51. D. Chu, D. J. Barnes, T. von der Haar, The role of tRNA and ribosome competition in coupling the expression of different mRNAs in *Saccharomyces cerevisiae*. *Nucleic Acids Res*. **39,** 6705-14 (2011). doi: 10.1093/nar/gkr300.

52. P. M. Caveney, S. E. Norred, C. W. Chin, J. B. Boreyko, B. S. Razooky, S. T. Retterer, C. P. Collier, M. L. Simpson, Resource Sharing Controls Gene Expression Bursting. *ACS Synth Biol*. **6**, 334-343 (2017). doi: 10.1021/acssynbio.6b00189.

53. Y. Liu, A code within the genetic code: codon usage regulates co-translational protein folding. *Cell Commun Signal*. **18**, 145 (2020). doi: 10.1186/s12964-020-00642-6.

54. P. S. Spencer, E. Siller, J. F. Anderson, J. M. Barral, Silent substitutions predictably alter translation elongation rates and protein folding efficiencies. *J Mol Biol*. **422**, 328-335 (2012). doi: 10.1016/j.jmb.2012.06.010.

55. E. P. O'Brien, M. Vendruscolo, C. M. Dobson, Kinetic modelling indicates that fast-translating codons can coordinate cotranslational protein folding by avoiding misfolded intermediates. *Nat Commun.***5**, 2988 (2014). doi: 10.1038/ncomms3988.

56. F. Trovato, E. P. O'Brien, Fast Protein Translation Can Promote Co- and Posttranslational Folding of Misfolding-Prone Proteins. *Biophys J*. **112**, 1807-1819 (2017). doi: 10.1016/j.bpj.2017.04.006.

57. C. L. Simms, L. L. Yan, H. S. Zaher, Ribosome Collision Is Critical for Quality Control during No-Go Decay. *Mol Cell*. **68**, 361-373.e5 (2017). doi: 10.1016/j.molcel.2017.08.019.

58. S. Juszkiewicz, G. Slodkowicz, Z. Lin, P. Freire-Pritchett, S. Y. Peak-Chew, R. S. Hegde, Ribosome collisions trigger cis-acting feedback inhibition of translation initiation. *Elife* **9**, e60038 (2020). doi: 10.7554/eLife.60038.

59. K. Saito, H. Kratzat, A. Campbell, R. Buschauer, A. M. Burroughs, O. Berninghausen, L. Aravind, R. Green, R. Beckmann, A. R. Buskirk, Ribosome collisions induce mRNA cleavage and ribosome rescue in bacteria. *Nature* **603**, 503-508 (2022). doi: 10.1038/s41586-022-04416-7.

60. E. Mordret, O. Dahan, O. Asraf, R. Rak, A. Yehonadav, G. D. Barnabas, J. Cox, T. Geiger, A. B. Lindner, Y. Pilpel, Systematic Detection of Amino Acid Substitutions in Proteomes Reveals Mechanistic Basis of Ribosome Errors and Selection for Translation Fidelity. *Mol Cell*. **75**, 427-441.e5 (2019). doi: 10.1016/j.molcel.2019.06.041.

61. M. Sun, J. Zhang, Preferred synonymous codons are translated more accurately: Proteomic evidence, among-species variation, and mechanistic basis. *Sci Adv*. **8,** eabl9812 (2022). doi: 10.1126/sciadv.abl9812.

62. P. Dave, G. Roth, E. Griesbach, D. Mateju, T. Hochstoeger, J. A. Chao. Single-molecule imaging reveals translation-dependent destabilization of mRNAs. *Mol Cell*. **83**, 589-606.e6 (2023). doi: 10.1016/j.molcel.2023.01.013.

63. V. Presnyak, N. Alhusaini, Y. H. Chen, S. Martin, N. Morris, N. Kline, S. Olson, D. Weinberg, K. E. Baker, B. R. Graveley, J. Coller. Codon optimality is a major determinant of mRNA stability. *Cell* **160**, 1111-24 (2015). doi: 10.1016/j.cell.2015.02.029.

64. L. Y. Chan, C. F. Mugler, S. Heinrich, P. Vallotton, K. Weis. Non-invasive measurement of mRNA decay reveals translation initiation as the major determinant of mRNA stability. *Elife* **7**, e32536 (2018). doi: 10.7554/eLife.32536.

65. K. Leppek, R. Das, M. Barna, Functional 5' UTR mRNA structures in eukaryotic translation regulation and how to find them. *Nat Rev Mol Cell Biol*. **19**, 158-174 (2018). doi: 10.1038/nrm.2017.103.

66. C. A. Charneski, L. D. Hurst, Positively charged residues are the major determinants of ribosomal velocity. *PLoS Biol.* **11**, e1001508 (2013). doi: 10.1371/journal.pbio.1001508.

67. R. Sabi, T. Tuller, Modelling the efficiency of codon-tRNA interactions based on codon usage bias. *DNA Res.* **21**, 511-526 (2014). doi: 10.1093/dnares/dsu017.

68. D. C. Liu, J. Nocedal, On the limited memory BFGS method for large scale optimization. *Mathematical Programming* **45**, 503–528 (1989).

69. S. Reuveni, I. Meilijson, M. Kupiec, E. Ruppin, T. Tuller, Genome-scale analysis of translation elongation with a ribosome flow model. *PLoS Comput Biol*. **7**, e1002127 (2011). doi: 10.1371/journal.pcbi.1002127.

70. L. J. Cook, R. K. Zia, B. Schmittmann, Competition between multiple totally asymmetric simple exclusion processes for a finite pool of resources. *Phys Rev E Stat Nonlin Soft Matter Phys*. **80**, 031142 (2009). doi: 10.1103/PhysRevE.80.031142.

71. C. A. Brackley, M. C. Romano, M. Thiel, The dynamics of supply and demand in mRNA translation. *PLoS Comput Biol.* **7**, e1002203 (2011). doi: 10.1371/journal.pcbi.1002203.

72. A. Jain, M. Margaliot, A. K. Gupta, Large-scale mRNA translation and the intricate effects of competition for the finite pool of ribosomes. *J R Soc Interface* **19,** 20220033 (2022). doi: 10.1098/rsif.2022.0033.

73. C. Miller, B. Schwalb, K. Maier, D. Schulz, S. Dümcke, B. Zacher, A. Mayer, J. Sydow, L. Marcinowski, L. Dölken, D. E. Martin, A. Tresch, P. Cramer, Dynamic transcriptome analysis measures rates of mRNA synthesis and decay in yeast. *Mol Syst Biol*. **7,** 458 (2011). doi: 10.1038/msb.2010.112.

74. J. V. Geisberg, Z. Moqtaderi, X. Fan, F. Ozsolak, K. Struhl, Global analysis of mRNA isoform half-lives reveals stabilizing and destabilizing elements in yeast. *Cell* **156**, 812-824 (2014). doi: 10.1016/j.cell.2013.12.026.

75. A. Belle, A. Tanay, L. Bitincka, R. Shamir, E. K. O'Shea, Quantification of protein half-lives in the budding yeast proteome. *Proc Natl Acad Sci USA* **103**, 13004-13009 (2006). doi: 10.1073/pnas.0605420103.

76. A. Garai, D. Chowdhury, T. V. Ramakrishnan, Fluctuations in protein synthesis from a single RNA template: stochastic kinetics of ribosomes. *Phys Rev E Stat Nonlin Soft Matter Phys*. **79**, 011916 (2009). doi: 10.1103/PhysRevE.79.011916.

77. A. Nishimura, M. Morita, Y. Nishimura, Y Sugino, A rapid and highly efficient method for preparation of competent Escherichia coli cells. *Nucleic Acids Res*. **18**, 6169 (1990). doi: 10.1093/nar/18.20.6169.

78. R. D. Gietz, R. H. Schiestl, High-efficiency yeast transformation using the LiAc/SS carrier DNA/PEG method. *Nat Protoc*. **2**, 31-34 (2007). doi: 10.1038/nprot.2007.13.

79. R. Higuchi, B. Krummel, R. K. Saiki, A general method of in vitro preparation and specific mutagenesis of DNA fragments: study of protein and DNA interactions. *Nucleic Acids Res.* **16**, 7351-7367 (1988). doi: 10.1093/nar/16.15.7351.

Acknowledgments

The authors are thankful to the members of the lab of Dr. Gayatri Mukherjee, School of Medical Science and Technology, IIT Kharagpur for help with flow cytometry.

Financial disclosure statement

This work was supported by funding from IIT Kharagpur ISIRD grant and Science and Engineering Research Board (SERB) grant ECR/2017/002328 to RD. The funders had no role in study design, data collection and analysis, decision to publish or preparation of the manuscript.

Author contributions

Conceptualization: RD

Methodology: SP, UR, RD

Investigation: SP, UR, RD

Visualization: SP, UR, RD

Funding acquisition: RD

Project administration: RD

Supervision: RD

Writing – original draft: SP, UR, RD

Writing – review & editing: SP, UR, RD

Competing interests

The authors have declared that no competing interests exist.

Data availability

Flow cytometry data are available in github:

https://github.com/riddhimandhar/TranslationModNoise

and dryad: https://doi.org/10.5061/dryad.tb2rbp06x

https://datadryad.org/stash/share/D8AhKWZIiouA5HNG9fjUytzetVlz_AOCagXsKcID0WI

Code availability

All codes for data analysis and models are available in github:
https://github.com/riddhimandhar/TranslationModNoise

Supplementary Materials

Figs. S1 to S21

Tables S1 to S3